HNPS Advances in Nuclear Physics

Vol 2 (1991)

HNPS1991

K-SHELL IONIZATION AND X-RAY PRODUCTION CROSS SECTIONS BY PROTONS IN VACUUM AND GASEOUS ENVIRONMENT

N. Kallithrakas-Kontos, A. A. Katsanos

doi: 10.12681/hnps.2854

K-SHELL IONIZATION AND X-RAY PRODUCTION CROSS SECTIONS BY PROTONS IN VACUUM AND GASEOUS ENVIRONMENT

N. KALLITHRAKAS-KONTOS and A. A. KATSANOS
Technical University of Crete, 73100 Chania, Greece

ABSTRACT

The K_α ionization and x-ray production cross sections from the bombardment of three metal targets with protons were measured in vacuum and in gaseous environment (external beam technique). Proton energies between 1.5 and 8 MeV were used. The experimental K shell ionization and x-ray production cross sections were calculated for the same targets and compared with three theoretical and two semiempirical approximations. For the measurements in gaseous environment the influence of the secondary electrons (delta electrons) emitted from the gas, to the x-ray yields was investigated. For this purpose a suitable model was introduced and tested experimentally.

1. INTRODUCTION

The inner shell ionization and x-ray production cross sections present theoretical as well as experimental interest, emphasized by the numerous publications which appear for different projectiles, energies and targets [1-3]. Still the list of the available data is far from complete, while differences up to 30% in the cross sections appear among the various investigators, indicating the need for additional and more accurate data. Furthermore, there is no report so far of the problem of projectile - atom interaction in the environment of a gas, a problem related to the practical application of the PIXE elemental analysis method with external beams.

Experimental data are usually compared with theoretical models in order to test the validity of their approximations. These models are the Plane Wave Born Approximation (PWBA), the Binary Encounter Approximation (BEA), and the Semiclassical Approximation (SCA). Beside these, two semiempirical models have been developed by Johansson [4] and Paul [5] for more accurate approach to the experimental data.

One practical use of the x-ray production cross sections concerns the Proton Induced X-ray emission (PIXE) spectroscopy. A very useful development of PIXE is the external beam technique [6] in which the target is bombarded by protons in gaseous environment (air or other gas). In that case the gas may produce enhancement effects to the characteristic x-ray yields, due primary x-rays and secondary electrons (SE)

emitted from the gas. This is an analogous effect to the thick target enhancement, which has already been studied in some cases. A major difference in the case of gas surrounding is that the SE which may affect the x-ray production, are produced from the whole mass of the gas, while the characteristic x-rays are produced only from a thin target, and this increases the enhancement effect (see section 2.3). On the other hand, the gas atomic number is usually lower than that of the target, excluding enhancement from the primary x-rays in this case.

The aim of the present work was the theoretical and experimental study of the secondary electron enhancement in the case of the gaseous atmosphere. Furthermore, additional data on x-ray production cross-sections are always useful, as mentioned earlier. For the above purpose the K_{α} x-ray production yields from the bombardment of thin metal targets with protons were measured in vacuum and in gaseous environment (external beam technique). Proton energies between 1.5 and 8 MeV were used. From the x-ray yields, the experimental K shell ionization and x-ray production cross sections were calculated for the same targets and compared with the calculations of three theoretical and two semiempirical approximations. Finally, a model was introduced for the theoretical calculation of the influence of the secondary electrons (delta electrons) emitted from the gas, to the characteristic x-ray yields. The results of these calculation are compared with the

obtained experimental data.

2. THEORY

2.1 General

The problem of the influence of the delta electrons to the x-ray production has only been faced in the case of thick target bombardment with protons. As "thick target" in this case, for a specific proton energy, is defined every target with thickness greater than the proton range. As "thin target" is defined any target that has no significant effect on the proton energy, referred to the x-ray production cross section across the proton path. The most significant results of such studies up to now are reviewed in section 2.2, while in section 2.3 a comparison between the case of thin targets in gaseous atmosphere and the thick target effect is presented. Finally, the calculations of the delta electrons enhancement are given in the section 2.4.

2.2 Thick target enhancement effects

In the PIXE analysis of trace elements inside a thick target, various enhancement effects to the produced x-rays may occur. These effects can be due to "secondary" excitations induced by: i) Primary induced x-rays, ii) secondary electrons, iii) bremsstrahlung radiation, iv) Auger electrons and by v) target-target collisions. From all these secondary effects only the first two may become important.

The enhancement from primary induced x-rays has already been studied in different cases and requires a matrix of higher atomic number than that of analysed trace element.

For excitation by secondary electrons, the more complete calculations are given by Van der Kam et al. [7], for different matrices and trace elements, and for initial proton energy (E_o) 2.5 MeV. These authors found an important enhancement in x-ray production, especially for the lower Z elements in higher Z matrices, but as they noticed, this enhancement may have been overestimated.

More realistic calculations have been performed by Folkman [8]. For scandium trace element and aluminium matrix, as an example, secondary electron excitation becomes important for $E_o > 4$ MeV. The calculations of Folkman for thick target analysis are also used by Raith et al. [9]

Calculations for 160 MeV protons on thick targets of gold and copper are given by Jarvis et al. [10], who examined the influence of the matrix to itself. They calculated enhancement of about 10% for copper and 30% for gold, and found good agreement with their experimental results. These calculations are also accepted by Akselsson et al. [11] for lower energies ($2.5 < E_o < 11$ MeV) and low Z elements ($21 < Z < 30$), resulting in a small increase of the cross section.

The conclusion is that the problem of secondary electron enhancement has not been yet completely solved theoretically, while there is a lack of experimental data for this effect.

2.3 Enhancement comparison between thick target and gaseous atmosphere

The schematic representation of the phenomena during the bombardment of a thin target in gaseous atmosphere is given in Fig. 1, ere the gas is divided into n thin (referred to electron energy loss) layers.

For comparison with the case of the thick target in vacuum, the gas may be considered as the first part of a thick target with the same surface density and atomic number, and divided in the same number of layers. An assumption that all electrons ejected from the gas have the same final energy is accepted at first. The percent enhancement E_g of the x-ray production in gas environment is given by the relation

$$E_g = 100 \cdot \frac{N_e(E_i) \cdot \sigma_e(E_i)}{\sigma_m}, \qquad (1)$$

where $N_e(E_i)$ is the number of electrons with the same final energy E_i produced per proton that reaches the target. $\sigma_e(E_i)$ the x-ray production cross section for these electrons and σ_m the x-ray production cross section for the proton.

In the thick target case the percent enhancement E_t is given by

$$E_t = 100 \frac{[N_{1e}(E_i) + N_{2e}(E_i) + \ldots + N_{ne}(E_i)] \cdot \sigma_e(E_i)}{n \cdot \sigma_m}, \qquad (2)$$

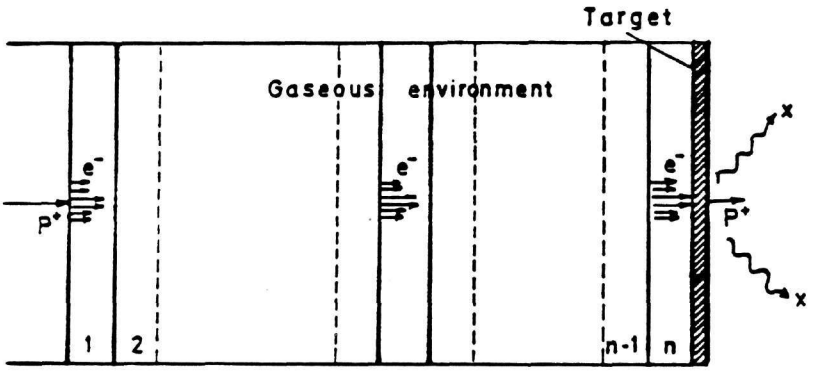

Fig. 1. A schematic representation of the phenomena during the bombardment of a thin target in gaseous environment.

where $N_{1e}(E_1)$, $N_{2e}(E_1)$, etc., represent the numbers of electrons produced per proton that reach the first, second etc. layers respectively with final electron energy E_1, when they reach the target; n is the number of thick target layers, which is equal with the number of the gas layers of Fig. 1. The proton cross section has been multiplied by n, because x-rays are produced by each of the n layers. In relation (2) only the last coefficient $N_{ne}(E_1)$ is equal with the $N_e(E_1)$ of relation (1), because only for the last layer the electrons come from the whole mass of the target; all the other coefficients are lower. For this reason it follows that

$$E_e < \frac{n.N_{ne}(E_1).\sigma_e(E_1)}{n.\sigma_p}$$

or

$$E_e < \frac{N_{ne}(E_1).\sigma_e(E_1)}{\sigma_p}$$

therefore

$$E_e < E_p. \qquad (3)$$

It has been accepted that all the electrons reaching the target have the same energy E_1. This assumption is not true, but the same relations hold for electrons with any final energy and therefore they hold for all electrons. Another assumption that has been made is that the first layer of the thick target is considered to have the same surface density with the gas. This part of the target is the most important, because the energy of the protons in the subsequent layers is

smaller and the effect is expected lower. Therefore relation (3) is not affected by the above assumptions and leads to the conclusion than the enhancement effect for thick target is lower than for the same effect caused by the gaseous environment.

2.4 Calculations of cross section enhancement in gaseous atmosphere

The percent enhancement of the x-ray production yield in gaseous atmosphere is defined by the relation

$$E = 100.X_e/X_p, \tag{4}$$

where X_p is the number of x-rays produced by protons and X_e the number produced by electrons. For a thin target

$$E = 100.N_e.\sigma_e/N_p.\sigma_p, \tag{5}$$

where σ_e and σ_p are the x-ray production cross sections by electrons and protons, and N_e, N_p the number of secondary electrons and protons that hit the target surface. If N_p is set equal to 1 and N_e will represent the number of secondary electrons produced per proton, in the gas.

The calculation of the enhancement is done in three steps. First the gas is divided in thin layers and for each layer the number of secondary electrons produced is calculated

per proton, as a function of the electron energy; in a second step the final energy of these electrons that reach the target is calculated and, third, by the number of x-rays produced by those electrons is derived. A computer program, named GAS, was written to produce these calculations. The calculations of the three steps are described in the next three paragraphs, respectively.

For the secondary electron production calculations the proton energy in every gas layer was defined from the known energy loss of protons [12]. For the number of produced electrons from each layer as a function of their energy, the differential cross section to the ejected electron energy by proton impact was needed. For this purpose, the BEA [13] with the Slater approach for the electron mean binding energy, was used. Some experimental differential cross section data are also available for different gasses, but there is lack of data for higher proton energies [14, 15]. The agreement between the existing data and the calculated values by the BEA has been examined for helium and argon gasses and the results are presented in tables 1 and 2. There is a discrepancy of the order of 30 % between theory and experiment, which is comparable with the recorded discrepancies in the x-ray production cross sections experimental values. The uncertainties of the experimental measurements are also about 25 %.

When the SE traverse the gas, they loose part of their energy due to collisions and bremsstrahlung emission. For

Table 1. Comparison between theoretical predictions of BEA [13] for differential to the energy cross sections for ejection of high energy SE, and experimental results [14] in helium. Ep is the incident proton energy, Ee the ejected electron energy and % difference the percent difference of theoretical minus experimen tal, to the theoretical cross section.

Ep(MeV)	Ee(KeV)	$d\sigma/dE(m^2/eV)$ (BEA)	$d\sigma/dE(m^2/eV)$ (Experimental)	% difference
1.0	1.000	0.234 E-25	0.258 E-25	-10
	1.500	0.102 E-25	0.119 E-25	-14
	2.000	0.412 E-26	0.482 E-26	-17
	2.500	0.209 E-27	0.225 E-27	-8
1.5	1.000	0.157 E-25	0.171 E-25	-8
	1.500	0.699 E-25	0.808 E-25	-13
	2.000	0.393 E-26	0.470 E-26	-16
	2.500	0.246 E-26	0.293 E-26	-16
	3.000	0.134 E-26	0.143 E-26	-6
	3.500	0.187 E-27	0.146 E-27	+28
4.2	1.166	0.412 E-26	0.335 E-26	+23
	1.359	0.304 E-26	0.232 E-26	+31

Table 2. Comparison between theoretical predictions of BEA [13] for differential to the energy cross sections for ejection of high energy SE, and experimental results [15] in argon. Ep is the incident proton energy, Ee the ejected electron energy and % difference the percent difference of theoretical minus experimen tal, to the theoretical cross section.

Ep(MeV)	Ee(KeV)	$d\sigma/dE(m^2/eV)$ (BEA)	$d\sigma/dE(m^2/eV)$ (Experimental)	% difference
2.0	1.000	0.635 E-25	0.880 E-25	-38
	1.500	0.288 E-25	0.375 E-25	-30
	2.000	0.163 E-25	0.231 E-25	-42
	2.500	0.103 E-25	0.152 E-25	-48
	3.000	0.700 E-26	0.893 E-26	-27
	3.500	0.476 E-26	0.571 E-26	-20
	4.000	0.294 E-26	0.221 E-26	+25
	4.500	0.682 E-27	0.480 E-27	+30
4.2	1.000	0.310 E-25	0.494 E-25	-38
	1.500	0.142 E-25	0.208 E-25	-32
	2.000	0.812 E-26	0.114 E-25	-29
	2.500	0.525 E-26	0.757 E-26	-31
	3.000	0.366 E-26	0.521 E-26	-30
	3.500	0.270 E-26	0.308 E-26	-12
	4.000	0.207 E-26	0.245 E-26	-16
	4.500	0.164 E-26	0.224 E-26	-27
	5.000	0.132 E-26	0.167 E-26	-21
	5.500	0.108 E-26	0.907 E-27	+19

electron energy 50 KeV the energy loss through bremsstrahlung is 3 orders of magnitude lower than through collisions. In our experiments the electrons had much lower energies and therefore even lower bremsstrahlung emission, so this type of energy loss could be neglected and the total loss was calculated by the Bethe formula, which is a very good approximation for $E_e > 1$ KeV [16]. Electrons below 1 KeV cannot ionize the inner shells of the target atoms, so they were ignored.

For the calculation of the angle of SE ejection two different approximations have been accepted in the bibliography [10]. The forward approximation, in which all the electrons are ejected at zero degrees relative to the proton beam and the isotropic one where isotropic distribution of SE ejection over a 2π solid angle is supposed. For the SE with KeV energies, which are of interest here, the forward approximation is more realistic, but calculations were performed with both models.

The ionization cross sections by electron impact were calculated using the Casnati et al. semiempirical formula [17]. For the proton ionization of the target atoms the semiempirical cross sections of Paul [5] were used. Ionization cross sections were used instead K_α x-ray production cross sections because their ratio is the same for electron and proton impact, as the fluorescence yields and the K_α/K_α ratios are independent of the mode of excitation (with the exception of heavy ion excitation). In the isotropic approximation the

solid angle that is defined by the point of SE production and the target area was calculated while in the forward approximation all SE reach the target.

3. EXPERIMENTAL

Protons in the range 1-8 MeV were obtained from the 10 MeV Tandem Van der Graaff accelerator of the NRCPS "DEMOKRITOS". The targets were mounted in an aluminium chamber, specially constructed for this purpose, at 45° angle to the incident beam, as shown in Fig. 2. Gasses of known pressure were fed into the chamber when gaseous atmosphere was required. Kapton foils of a 1.2 mg/cm^2 in thickness were used as exit windows for the protons and the produced x-rays. For vacuum bombardment, the proton exit foil was omitted. The diameter of the beam was 3 mm and the current was always kept below 6 nA, in order to avoid target heating. The proton current was monitored at the chamber and the proton exit foil together and integrated to give the total proton charge. This charge was between 0.50 and 1.00 μC.

A Ge(in) solid state detector with 150 eV resolution at 5.9 KeV was placed at 90° relative to the beam and collimated with a 5 mm in diameter lead collimator. The distance between the target and the surface of the detector was 7.0 cm. The efficiency of the detector vs. energy was measured using thin foils with standard thickness (from Micromatter), as well as thick foils.

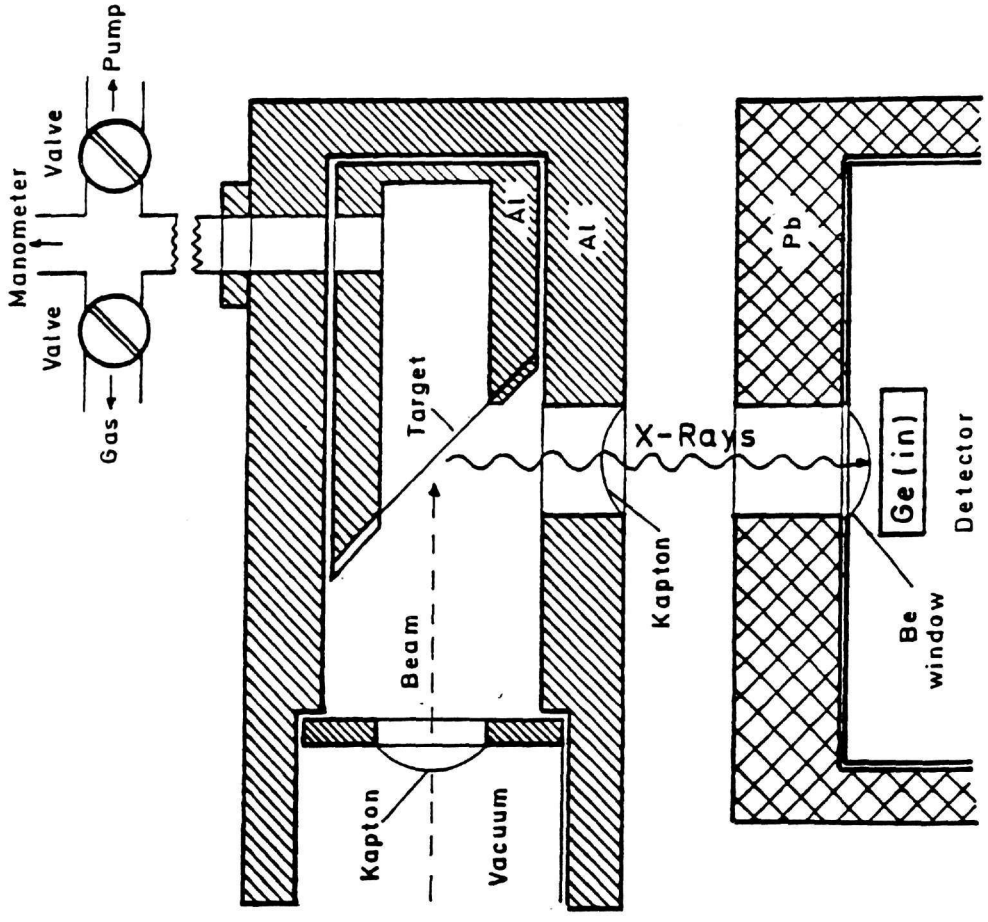

Fig. 2. Experimental setup for the bombardment of thin targets in vacuum and gaseous atmosphere.

The targets were prepared by evaporation of metals on Kapton foils of 1.2 mg/cm^2 thickness. The target selection was based on the following criteria: Targets with low atomic number were preferred for higher ionization probability of the inner shells by the SE. At the same time the atomic number should be higher than 18 in order to avoid fluorescence by the argon x-rays. These conditions let to calcium (in the form of calcium fluoride), metallic titanium and iron. Potassium was excluded because of the high background from the argon peak in the vicinity.

Data collection and analysis were prepared with a computer based analysis system. Dead time corrections were made with the aid of a pulser coupled through the preamplifier and it was always kept below 10 % to avoid pile up peaks.

4. RESULTS

4.1 Cross sections in vacuum

The obtained K-shell ionization (σ_{iK}), and the K and K_α production cross sections (σ_{KK}, $\sigma_{K\alpha}$) in vacuum, are presented in tables 3, 4 and 5 for the elements calcium, titanium and iron, respectively, for different proton energies. Three or four measurements of the K_α x-rays for each element and proton energy were taken in order to check the reproducibility of the method. The K-shell x-ray production cross sections were calculated from the known values of K_α/K_α ratios [18] and the K-shell ionization cross sections with the use of fluorescence

Table 3. K_α and K x-ray production, and K ionization cross sections (in barns) for calcium in vacuum, as a function of proton energy (E_p). The experimental uncertainties are 8% for $\sigma_{K\alpha}$, $\sigma_{K\beta}$, and 9% for σ_{iK}.

E_p	$\sigma_{K\alpha}$	$\sigma_{K\beta}$	σ_{iK}
2.0	212	239	1466
2.5	291	328	2012
3.0	357	403	2472
4.0	473	534	3276
5.0	555	626	3840
5.5	559	631	3871
6.0	494	557	3417

Table 4. K_α and K x-ray production, and K ionization cross sections (in barns) for titanium in vacuum, as a function of proton energy (E_p). The experimental uncertainties are 7% for $\sigma_{K\alpha}$, $\sigma_{K\beta}$, and 8% for σ_{iK}.

E_p	$\sigma_{K\alpha}$	$\sigma_{K\beta}$	σ_{iK}
1.5	96	109	509
2.5	225	255	1192
3.0	283	321	1500
3.5	333	378	1766
4.0	380	431	2014
4.5	421	477	2229
5.0	442	501	2341
5.5	463	525	2453
6.0	486	551	2575
6.5	501	568	2654
7.0	510	578	2701
7.5	530	601	2808
8.0	535	607	2836

yields [19]. The total error is less than 10 % and the main sources are the uncertainties from the target thickness, solid angle of detection, x-ray absorption and the efficiency of the detector.

In Figs. 3 and 4 the K_α x-ray production cross sections are plotted as a function of proton energy. In the same figures the results of three theoretical and two semiempirical models for the same targets are also plotted. The three theoretical models are the PWBA with corrections for Coulomb repulsion, binding and relativity effects [20], the SCA with Coulomb correction [21] and the BEA with Coulomb correction [22, 23]. The two semiempirical models are the model of Johansson [4] and the model of Paul [5].

4.2 Cross sections in gas environment

The results of the predictions for the cross section enhancement of calcium, titanium and iron, calculated as described in section 2.4 are presented in Fig. 5 as a function of proton energy. These calculations were made with the forward approximation for the SE angle distribution, which is recognised as more realistic. The calculations were made for two gasses (argon and helium), proton energies from 2 to 10 MeV and for the setup used in our experiment (Fig. 2). A comparison between the Folkman predictions for enhancement in thick targets and our results (correspondence: thick target matrix - gas, thick target trace elements - thin target) is

Table 5. K_α and K x-ray production, and K ionization cross sections (in barns) for iron in vacuum, as a function of proton energy (E_p). The experimental uncertainties are 7% for $\sigma_{K\alpha}$, $\sigma_{K\beta}$, and 8% for σ_{iK}.

E_p	$\sigma_{K\alpha}$	$\sigma_{K\beta}$	σ_{iK}
1.5	39.8	45.2	133
2.5	110	126	371
3.0	146	166	488
3.5	183	207	609
4.0	219	249	732
4.5	254	289	850
5.0	269	306	900
5.5	302	343	1009
6.0	319	363	1068
6.5	338	383	1126
7.0	350	398	1171
7.5	367	417	1226
8.0	372	422	1241

Table 6. Comparison between the Folkman [8] predictions of enhancement in thick targets caused by SE (THICK), and our calculations for the corresponding bombardment of thin targets in gas surrounding (GAS), as a function of proton energy. Aluminium is supposed as the matrix element (or "gas") where Z represents the atomic number of the x-ray emitting element. The numbers are percent enhancements.

	2 MeV		3 MeV		4 MeV		6 MeV		8 MeV	
Z	THICK	GAS	THICK	GAS	THICK	GAS	THICK	GAS	THICK	GAS
11	2.2	13	5.4	25	9.6	40	20	82	32	145
13	1.2	6.3	3.6	13	6.8	20	15	38	26	61
15	0.54	3.0	2.1	7.7	4.6	12	12	22	20	34
18	0.12	0.62	0.79	3.3	2.2	6.3	7.1	12	14	18
21	0.03	0.11	0.20	0.97	0.86	2.8	3.9	6.8	8.9	10
25	0.01	0.02	0.03	0.11	0.15	0.62	1.4	3.1	4.3	5.7
29	-	0.01	0.01	0.02	0.03	0.08	0.32	0.97	1.6	2.8
35	-	-	-	-	0.01	0.01	0.03	0.05	0.18	0.46

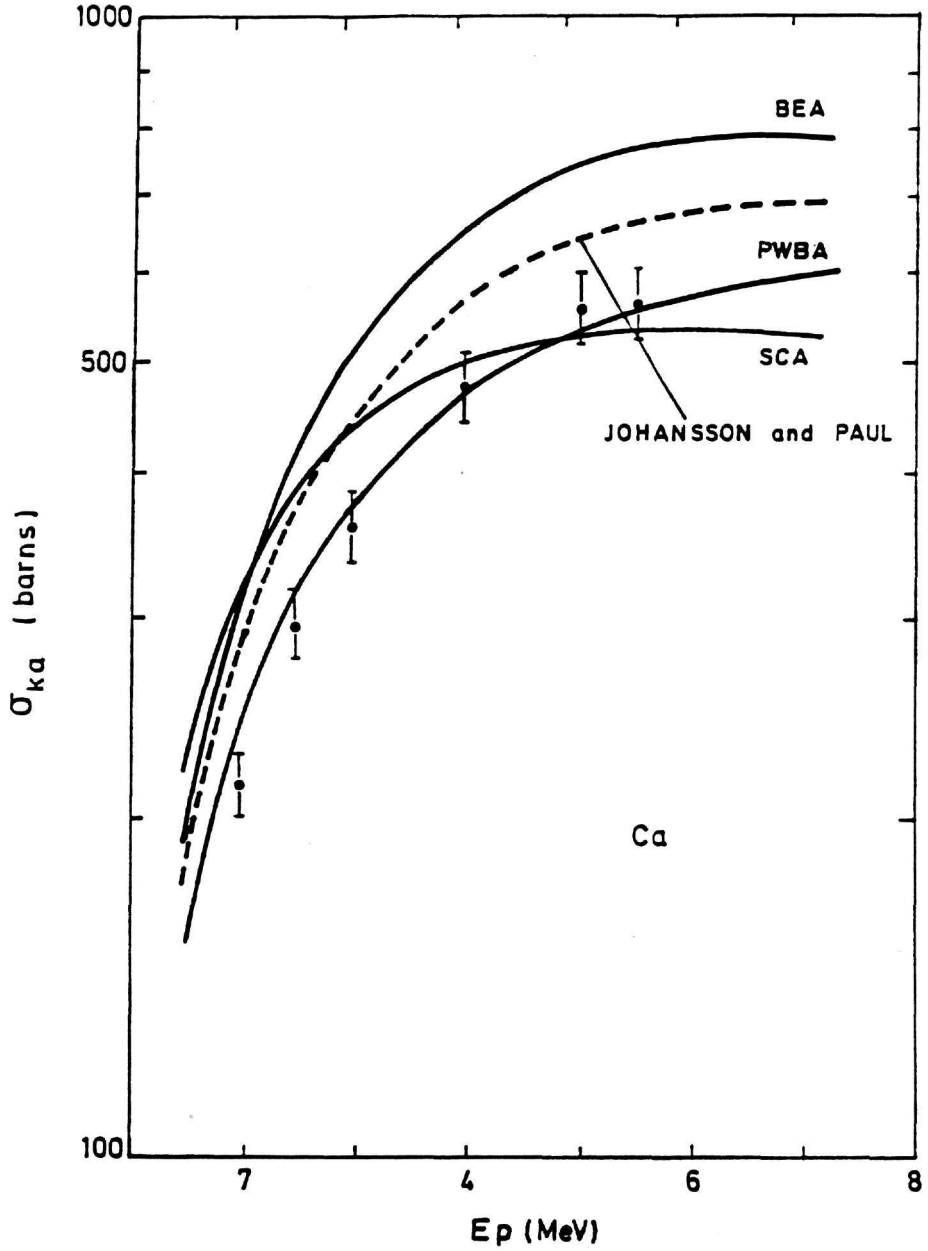

Fig. 3. Experimental K_α x-ray production cross sections for calcium, as a function of proton energy. The results of the BEA, PWBA and SCA theoretical models, and of the semiempirical ones of Paul and Johansson are also shown.

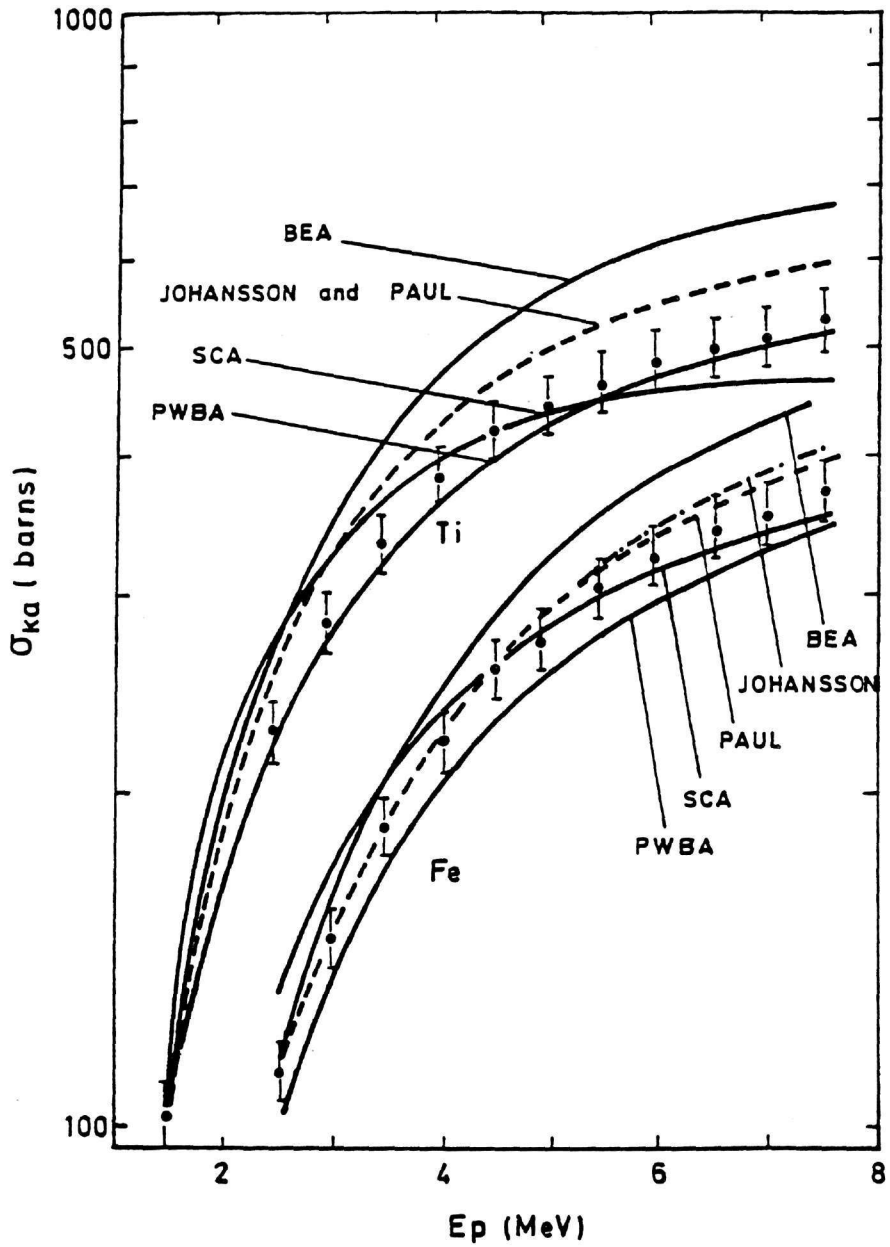

Fig. 4. Experimental K_α x-ray production cross sections for titanium and iron, as a function of proton energy. The results of the BEA, PWBA and SCA theoretical models, and of the semiempirical ones of Paul and Johansson are also shown.

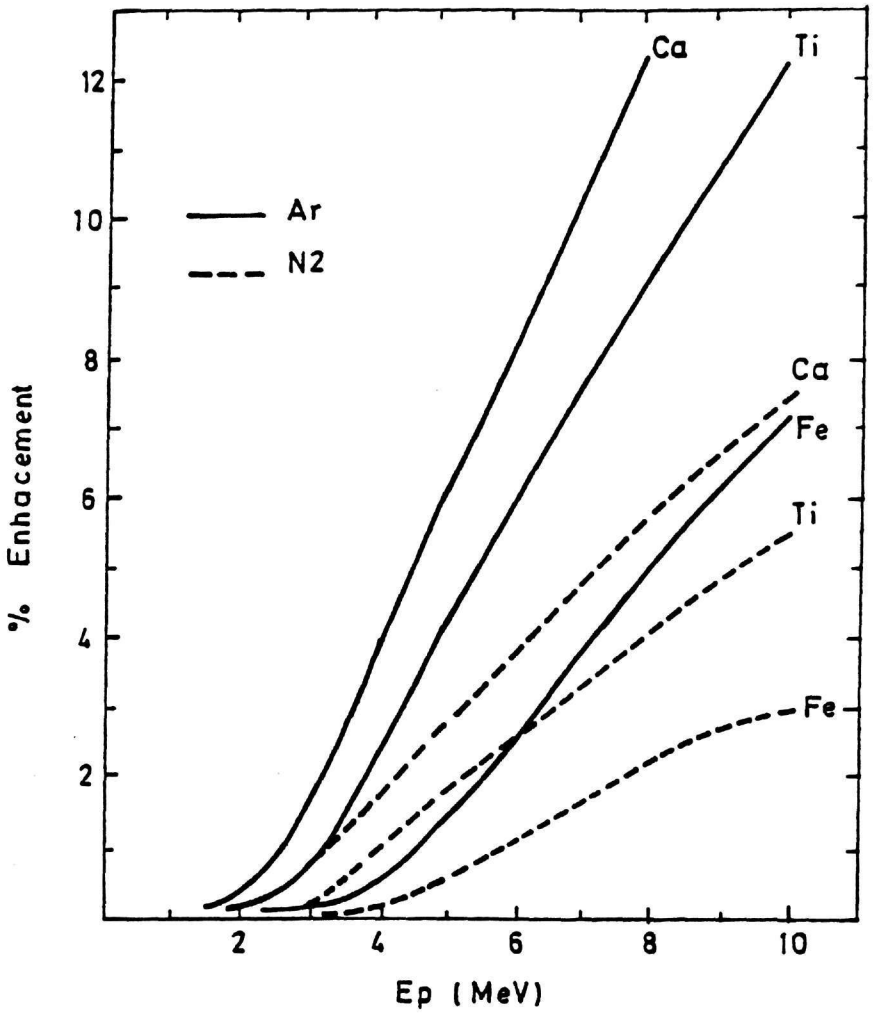

Fig. 5. Theoretical enhancements for thin target bombardment in gaseous atmosphere as calculated for different proton energies, three targets (Ca, Ti, Fe), and two gasses (N₂, Ar). The forward approximation of the secondary electron ejection has been assumed here.

presented in table 6. As predicted in section 2.3 the gas environment gives higher enhancements.

After the bombardment in vacuum, a thin film of Kapton foil was inserted in the beam path and a new series of in vacuum measurements was taken. As expected from the calculations, no measurable effect from the inserted Kapton foil in the yields was observed. In the next step, gasses were introduced into the chamber for the measurements in gaseous environment. In the case of helium, no measurable differences were found for all targets. The x-ray yields of the measurements in nitrogen environment, along with the results of the corresponding measurements in vacuum are shown in Fig. 6, as well as our theoretical calculations. The experiment of calcium in argon atmosphere was not successful because of the high background from the argon characteristic x-rays in the vicinity of the calcium emission. Measurements in argon environment were possible for titanium and iron and their cross sections in vacuum and argon environment, along with our theoretical predictions are also given in Fig. 6.

The main sources of errors are the same for the bombardment in vacuum and in gas surrounding (thickness of target, efficiency, solid angle), therefore the relative error for the two series of measurement (in vacuum and gas) is 1% and can not be plotted in the figures.

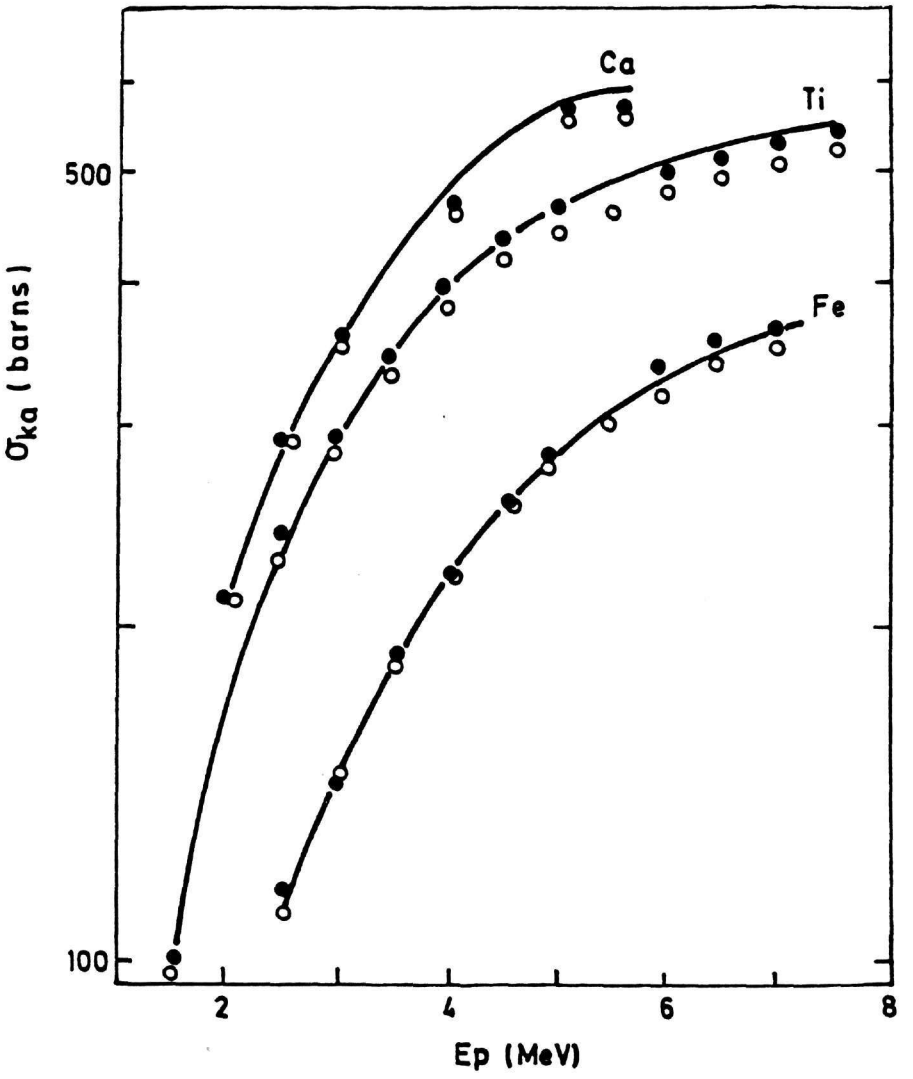

Fig. 6. Experimental Kα x-ray production cross sections for calcium, titanium and iron in vacuum (open circles) and gaseous atmosphere (black circles), as a function of proton energy. The gas is nitrogen for calcium and argon for titanium and iron. The predictions of this work for cross sections in gaseous atmosphere are also shown (continuous curves).

5. DISCUSSION

The experimental results for the cross sections in vacuum and the two theoretical models (BEA, PWBA) produce the same slope of the cross sections as a function of proton energy. The absolute values, however, predicted by BEA are higher, while the PWBA gives values closer to the experiment. The PWBA is a better approximation for the proton energies and the targets used. Good results can also be obtained from the BEA and the two semiempirical models if a experimentally defined correction factor is introduced

The bombardment with protons in gaseous environment proved that of low proton energies (below 3 MeV) and for target atomic numbers greater than 18 the x-ray enhancement from SE can be neglected. As these are the standard conditions that are usually used in the external beam PIXE, this means that no SE enhancement problems occurs in this widely used method. For higher proton energies and atomic numbers of gasses a SE enhancement is measurable but these conditions are rarely used in PIXE.

The theoretical calculations of the SE enhancement were found in good agreement with the experimental results, although there is an overestimation of the enhancement in higher proton energies and lower atomic numbers of targets. The most serious problem in the calculations is the lack of experimental data for differential to the energy cross sections for producing SE with energies greater than 1 KeV. The

BEA has been extrapolated to higher SE energies in our case and this could be another source of errors. As it can be seen from tables 1 and 2 the results of BEA are on the average in satisfactory agreement with the existing data, but there is an underestimation at low SE energies and an overestimation at the higher SE energies. Another reason for the differences may be the acceptance of the forward SE ejection.

Among the published calculations for the SE enhancement in thick targets Folkman gives the better results. Our results for the enhancements in gas environment are the upper limits for thick targets and can not been exceeded.

REFERENCES

[1] R.K. Gardner and Tom J. Gray, Atom. Data and Nucl. Data Tables 21 (1978) 515.

[2] H. Paul and J. Sacher, Atom. Data. and Nucl. Data Tables 42 (1989) 105.

[3] H. Paul, Atom. Data and Nucl. Data Tables, 24 (1979) 243.

[4] S.A.E. Johansson and T.B. Johansson, Nucl. Instr. and Meth. 137 (1976) 473.

[5] H. Paul, Nucl. Instr. and Meth. B3 (1983) 5.

[6] A. Katsanos, A. Xenoulis, A. Hadjiantoniou and R.W. Fink, Nucl. Instr. and Meth. 137 (1976) 119.

[7] P.M.A. Van Der Kam, R.W. Vis and H. Verheul, Nucl. Instr. and Meth. 142 (1977) 55.

[8] F. Folkman, Material Characterization using ion beams. Plenum Press (1978) 270.

[9] B. Raith, A. Stratmann, H. R. Wilde, B. Consior, S. Bruggerhoff and E. D. Jackwerth, Nucl. Instr. and Meth. 181 (1981) 199.

[10] O. N. Jarvis, C. Whitehead and M. Shah, Phys. Rev. A5 (1972) 1198.

[11] R. Akselsson and T. B. Johansson, Z. Physik 266 (1974) 245.

[12] H. H. Andersen and J. F. Ziegler, Hydrogen Stopping Powers and Ranges in All Elements, Plenum Press (1977) New York.

[13] M. E. Rudd, D. Gregoire and J. B. Crooks, Phys. Rev. A3 (1971) 1635.

[14] M. E. Rudd, L. H. Toburen and N. Stolterfoht, Atom. Data and Nucl. Data Tables 18 (1976) 413.

[15] M. E. Rudd, L. H. Toburen and N. Stolterfoht, Atom. Data and Nucl. Data Tables 23 (1979) 405.

[16] F. Rohrlich and B. C. Carlson, Phys. Rev. 93 (1954) 38.

[17] E. Casnati, A. Tartari and C. Baraldi, J. Phys. B: Atom. Mol. Phys. 15 (1982) 155.

[18] S. I. Salem, S. L. Panossian and R. A. Krause, Atom. Data and Nucl. Data Tables 14 (1974) 91.

[19] M. O. Krause, J. Phys. Chem. Ref. Dat., 8 (1979) 307.

[20] G. Basbas, Phys. Rev. A17 (1978) 1655.

[21] J. M. Hansteen, O. M. Johnsen and L. Kocbach, Atom. Data and Nucl. Data Tables 15 (1975) 305.

[22] J. S. Hansen, Phys. Rev. A8 (1973) 822.

[23] J. H. McGuire and K. Omidvar, Phys. Rev. A10 (1974) 182.